HHS Public Access

Author manuscript

Int J Pharm. Author manuscript; available in PMC 2024 November 25.

Published in final edited form as:

Int J Pharm. 2023 November 25; 647: 123547. doi:10.1016/j.ijpharm.2023.123547.

Microneedle-mediated transdermal delivery of N-acetyl cysteine as a potential antidote for lewisite injury

Sharvari Kshirsagar[a], **Amruta Dandekar**[a], **Ritesh K Srivastava**[b], **Jasim Khan**[b], **Suhail Muzaffar**[b], **Mohammad Athar**[b], **Ajay K. Banga**[a]

[a]Center for Drug Delivery Research, Department of Pharmaceutical Sciences, College of Pharmacy, Mercer University, Atlanta, Georgia, USA

[b]UAB Research Center of Excellence in Arsenicals, Department of Dermatology, University of Alabama at Birmingham, Birmingham, Alabama, USA

Abstract

Lewisite is a chemical warfare agent intended for use in World War and a potential threat to the civilian population due to presence in stockpiles or accidental exposure. Lewisite-mediated skin injury is characterized by acute erythema, pain, and blister formation. N-acetyl cysteine (NAC) is an FDA-approved drug for acetaminophen toxicity, identified as a potential antidote against lewisite. In the present study, we have explored the feasibility of rapid NAC delivery through transdermal route for potentially treating chemical warfare toxicity. NAC is a small, hydrophilic molecule with limited passive delivery through the skin. Using skin microporation with dissolving microneedles significantly enhanced the delivery of NAC into and across dermatomed human skin in our studies. Microporation followed by application of solution (poke-and-solution) resulted in the highest in vitro delivery (509.84 ± 155.04 μg/sq.cm) as compared to poke-and-gel approach (474.91 ± 70.09 μg/sq.cm) and drug-loaded microneedles (226.89 ± 33.41 μg/sq.cm). The lag time for NAC delivery through poke-and-solution approach (0.23 ± 0.04 h) was close to gel application (0.25 ± 0.02 h), with the highest for drug-loaded microneedles (1.27 ± 1.16 h). Thus, we successfully demonstrated the feasibility of rapid NAC delivery using various skin microporation approaches for potential treatment against lewisite-mediated skin toxicity.

Graphical Abstract

Corresponding Author: Dr. Ajay K. Banga, 3001 Mercer University Drive, Atlanta, GA 30341, United States, banga_ak@mercer.edu, Tel: +1 678 547 6423.

7.Author contributions

Sharvari Kshirsagar: Conceptualization, Data curation, Formal Analysis, Methodology, Software, Writing-original draft
Amruta Dandekar: Conceptualization, Formal Analysis, Validation, Writing- review and editing
Ritesh K Srivastava: Investigation, Writing-review and editing
Jasim Khan: Writing- review and editing
Suhail Muzaffar: Writing- review and editing
Mohammad Athar: Funding acquisition, Project administration, Writing- review and editing
Ajay K. Banga: Funding Acquisition, Project Administration, Supervision, Writing- review and editing

9.Conflict of interest

The authors declare no conflict of interest.

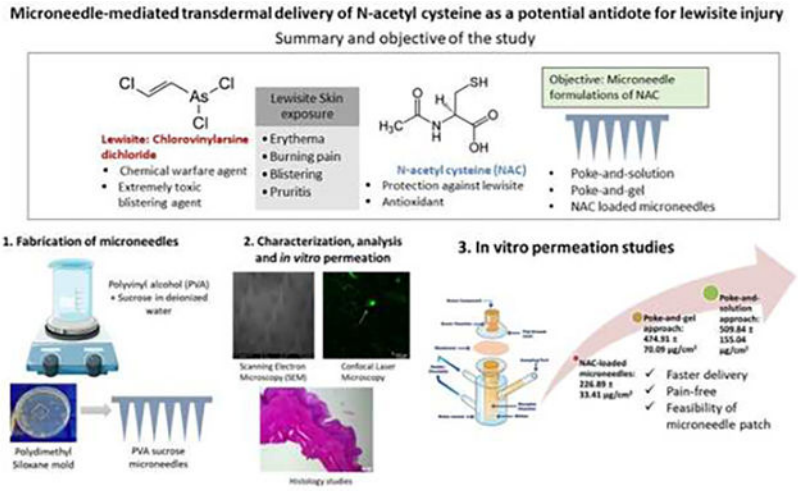

Keywords

N-acetylcysteine; microneedle; transdermal delivery; Lewisite; skin injury; antidote delivery

1. Introduction

Arsenicals are highly toxic chemical derivatives of arsenic that produce both acute and delayed damage to the tissues upon exposure(Li et al., 2016a). Lewisite is an arsenical-based chemical warfare agent that was initially created in 1918 to be used in World War I but remains in stockpiles in different countries (Centers for Disease Control and Prevention, 2018; National Institute of Health, 2007). The chemical nomenclature of Lewisite is chlorovinylarsine dichloride or dichloro(2-chlorovinyl)arsine (NIOSH and CDC, 2011). Lewisite has the property to produce severe chemical burns when it comes in direct contact with skin and/or any tissue (Watson and Griffin, 1992). It is a highly potent blistering agent. Upon exposure in lower concentrations, it causes skin and eye irritation along with respiratory tract irritation. However, at higher concentrations and broader exposure, it leads to the simultaneous blistering of multiple tissues (Li et al., 2016b). Studies report that exposure to Lewisite is highly toxic to the skin as it causes an immediate burning sensation, and observation of erythema within 30 minutes of exposure, followed by edema and blistering (Flora et al., 2009). The overall time required by the skin to recover from lewisite exposure without any treatment is around four weeks (Li et al., 2016a). Thus, it is essential to mitigate the painful skin injury caused by these and similar arsenic derivatives to reduce pain, inflammation, and blistering. Presently, the only FDA-approved antidote against lewisite-induced poisoning is 2,3-dimercapto-1-propanol, commonly known as British Anti-Lewisite (BAL)(Fox et al., 2021). Topical administration of BAL has been previously demonstrated to have some effectiveness in lowering the severity of skin lesions, but only when applied topically immediately after Lewisite exposure (National Institute of Health, 2007). However, BAL causes toxicity and often requires painful intravenous or intramuscular administration (Mouret et al., 2013). Our previous study with phenyl arsine oxide (PAO), a surrogate of Lewisite, explored decontamination strategies to attenuate

such damage (Vora et al., 2022a). N-acetyl cysteine (NAC) is an antioxidant reported to have a protective effect against lewisite-mediated injury (Li et al., 2016b). Our earlier studies suggest that NAC blocks the lewisite-mediated reactive oxygen species (ROS) due to its antioxidant activity. It increases the biosynthesis of glutathione, which can bind to the arsenicals to increase their excretion from the body (Delnomdedieu et al., 1993), thereby resulting in attenuation of skin injury due to lewisite toxicity(Li et al., 2016b). Thus, transdermal delivery of NAC can serve as a potential antidote treatment for arsenical skin injury. An ideal molecule for passive transdermal absorption is traditionally required to be low molecular weight, potent, and moderately lipophilic(Banga, 2011), which can be eventually formulated as a drug-in-adhesive transdermal patch(Vora and Banga, 2022). However, NAC has a molecular weight of 163.19 g/mol and a log P of −0.711, indicating that it is a hydrophilic molecule(ChemAxon, 2022). Due to its high aqueous solubility (ChemAxon, 2022), the passive transdermal delivery of NAC is challenging. As a result, several physical enhancement techniques, such as microneedle treatment (Junaid and Banga, 2022) or iontophoresis (Vora et al., 2022b) can be employed to disrupt the stratum corneum and enhance the delivery of highly hydrophilic drugs(Aldawood et al., 2021). We have previously demonstrated the use of chemical enhancers as well as iontophoresis to enhance the delivery of NAC through the skin (Dandekar et al., 2023). Amongst these techniques, skin microporation is a painless, minimally invasive, promising approach for drug delivery. Microneedles are micron-sized needles, typically less than 1 mm in length, that facilitate the delivery of hydrophilic molecules into and across the skin (Banga, 2009). Microneedles have several advantages, such as they are painless as compared to painful intravenous injections and can be self-administered(Giudice and Campbell, 2006). Microneedles are categorized as solid, coated, dissolving, and hollow microneedles(Guillot et al., 2020). Dissolving microneedles are designed to rapidly release the drug upon insertion in the skin and is desirable for quick onset of action (Xiu et al., 2022). In the present study, we have explored, for the first time, various skin microporation approaches using dissolving microneedles, such as microporation followed by application of the formulation, as well as drug-loaded microneedles to deliver NAC into and across the skin.

2. Materials and Methods

2.1 Materials

N-acetylcysteine, carboxymethyl cellulose sodium salt (CMC, low viscosity), and polyvinyl alcohol (PVA)(Parteck® MXP) were purchased from Sigma Aldrich (St. Louis, MO, USA). Sucrose was procured from Fisher Scientific (NJ, USA). Methylene blue was obtained from Sigma Aldrich (St. Louis, MO, USA), and Fluoresoft-0.35%® was purchased from Holles Laboratories Inc (Cohasset, MA, USA). Metal microneedles used as master templates were bought from Micropoint Technologies Pte Ltd (Pioneer Junction, Singapore). Sylgard®186 silicone elastomer and its curing agent were obtained from Dow Corning Corp. (MI, USA). Phosphate buffered saline (PBS) (10X, pH 7.4 ± 0.1) was bought from Fisher Scientific (Fisher BioReagents, NJ, USA). All solvents, such as methanol, ethanol, and acetonitrile, were High-Performance Liquid Chromatography (HPLC) grade from Pharmaco-aaper (Brookfield, CT, USA). Dermatomed Human skin (under a protocol exempted by Mercer

University Institutional Review Board (H0303041)) was obtained from a skin bank (New York Fire Fighters, NY, USA).

2.2 Methods

2.2.1 Preparation of polydimethylsiloxane (PDMS) molds for the fabrication of microneedles—PDMS molds were prepared using a method previously reported by our lab (Kshirsagar et al., 2022). Briefly, Sylgard® 186 silicone elastomer base and curing agent were weighed in a 10:1 w/w ratio. Metal microneedles consisting of a 10 × 10 array of stainless, pyramid-shaped microneedles with a height of 500 μm and a base of 150 × 150 μm along with a 500 μm pitch were used as master structures. The mixture of elastomer and curing agent was added to the metal microneedles, which were placed in a six-well plate. Air bubbles from the molds were removed using a vacuum, followed by heat curing at 90°C for 3 h.

2.2.2 Formulation of NAC solution—NAC was dissolved in 1 X PBS in a concentration of 15.96% w/w to form a clear solution. The formulated solution was characterized by visual observation and pH measurement. The formulated solution was used for poke-and-solution type of *in vitro* permeation studies.

2.2.3 Formulation of NAC-loaded gel—The NAC-loaded hydrogel was prepared by first dissolving 15.96% w/w of NAC in deionized water. Carboxymethylcellulose sodium salt (CMC) was added to the solution to form a 10% w/w gel of NAC. The gel was characterized for pH and rheological parameters and used for poke-and-gel application type of *in vitro* permeation studies.

2.2.4 Fabrication of placebo microneedles—Polyvinyl alcohol, Parteck® MXP, and sucrose were used for the preparation of dissolving polymeric microneedles. Initially, sucrose (20% w/w) was dissolved in deionized water at room temperature to form a clear solution. PVA (26.6% w/w) was slowly added to the solution of sucrose and deionized water. The solution blend was placed on a vertical rotary shaker at 30 rpm overnight to hydrate and form a homogenous polymer blend. 100 μL of the polymer blend was initially added to the PDMS mold. The mold was subjected to vacuum for 5 min to pull the solution inside the cavities to form the needles (Vacufuge Plus, Eppendorf). Next, the base of the microneedles was prepared by adding a further 100 μL of the polymer solution to the mold). The microneedle molds were placed in a desiccator for drying for seven days.

2.2.5 Fabrication of drug-loaded microneedles—As we aimed to formulate NAC-loaded microneedles with maximum drug loading for both immediate and sustained delivery of NAC, it was loaded in microneedle tips as well as the base. An excess N-acetyl cysteine was dissolved in deionized water and kept on a platform shaker at 150 rpm overnight to get a saturated solution. The solution was centrifuged at 4000 rpm at 25°C for 15 min to precipitate the undissolved NAC. The supernatant solution was collected and filtered through a 0.22 μm nylon syringe filter. This was followed by the addition of sucrose and PVA in a similar manner, as explained in the fabrication of blank microneedles

to form NAC-loaded microneedles. The NAC-loaded microneedles were subjected to characterizations along with drug content to determine the maximum drug loading.

2.2.6 Skin pre-treatment with the application of microneedles—Dermatomed human skin was removed from the freezer at −80°C. The unopened bag of skin was placed in a Ziploc bag and thawed in a water bath at 37 °C. Upon thawing, the skin was dried and cut into appropriate sizes for the in vitro permeation studies. The average thickness of the skin used for the permeation studies was 406.67 + 47.44 μm. Placebo/NAC-loaded microneedles were applied on the central portion of the skin piece using a thumb with moderate pressure for 2 min to facilitate microporation. This microporated skin piece was further used for characterization and permeation studies. In the case of permeation studies, care was taken to ensure that the microporated area matches the permeation area of the skin.

2.2.7 Characterization studies

2.2.7.1 Rheological characteristics: The rheology of the NAC gel was determined using a modular compact rheometer (MCR-302, Anton Paar USA Inc., Ashland, VA, USA). A complete flow curve of the shear stress or viscosity vs. shear rate was conducted. Multiple data points across a range of achievable shear rates were considered until plateaus were observed. An amplitude sweep test was performed to describe the deformation behavior of the gel. The results of the amplitude sweep test were presented as shear stress or strain on the x-axis and the storage and loss modulus on the y-axis, both in logarithmic scale.

2.2.7.2 Scanning electron microscopy (SEM): The size, shape, and appearance of the microneedles were measured through SEM. The ImageJ software was used to measure the needle length, base dimension, and needle-to-needle distance (National Institutes of Health, Bethesda, Maryland, USA) (n = 10). The microchannels created by the needles on the skin surface were visualized as well.

2.2.7.3 Skin integrity test: The skin integrity test was used to provide evidence of successful microporation of the skin by the microneedles. It was measured using a drop in the skin's electrical resistance. The resistance of the skin was measured using a procedure previously used by our lab (Shrestha and Banga, 2022). Briefly, a silver/silver chloride electrode assembly was coupled to a waveform generator and a digital multimeter (Agilent Technologies, Santa Clara, CA). Dermatomed skin was mounted on Franz diffusion cells with the stratum corneum facing up, and 5 mL of 10 mM PBS was placed in the receptor compartment. After that, 300 μL of 10 mM PBS was added to the donor chamber; the skin tissue was allowed to acclimate for 15 minutes. An alternating electrical current with a voltage of 90 mV at 10 Hz was passed through a skin sample with an area of 0.64 sq.cm to determine the skin's electrical resistance. The voltage drop (V) across the skin was measured, and the values of skin electrical resistance were determined using the equation below.

$$RS = VS\,RL / (VO - VS)$$

Where the load resistor (RL) was 100 kΩ, and voltage Vo was 100 mV. All the experiments employed skin samples with a resistance of at least 10 kΩ prior to microneedle application. Typically, a decrease in electrical resistance is observed after skin microporation using microneedles due to the formation of hydrophilic microchannels, which reduces the barrier integrity of the skin.

2.2.7.4 Histology Studies of the microporated skin: According to the method we previously explained in our earlier study (Dandekar et al., 2022a), histological examinations were conducted on intact and microporated dermatomed human skin to confirm the microporation ability of fabricated microneedles. These samples were frozen at −80°C in a Tissue-Tek stub containing an Optical Coherence Tomography compound medium. Using a Leica CM1860 cryostat (Leica Biosystems Nussloch GmbH, Germany), the frozen tissues were then sectioned at −20°C. The microchannels were visualized using a Leica DM 750 microscope, 10 μm thick sections were first stained with methylene blue (1% w/v). The sections were further stained with hematoxylin and eosin and examined under an optical microscope at a magnification of 20X.

2.2.7.5 Confocal laser microscopy studies: Studies using confocal laser microscopy measured the depth of microchannels formed upon application of the PVA sucrose microneedles. Fluoresoft 0.35%® solution was used to illuminate the microporated area of the skin that had undergone microporation. The observation was conducted using a computerized Leica SP8 confocal microscopy system (Leica Microsystems, GmbH, Germany). To determine the total depth of the microchannels, a Z-stack with a system-adjusted step count of 10 μm was generated.

2.2.7.6 Mechanical strength test: The resistance of microneedles to the application of increasing axial forces depends critically on the mechanical strength of the microneedles. Using a Stable Micro Systems TA.XT Express Texture Analyzer (Texture Technologies Corp., South Hamilton, MA, USA), the mechanical strength of microneedles was assessed. A single microneedle array with needles facing upward was positioned for the process on the analyzer's base plate. The Texture Analyzer was equipped with a stainless-steel probe with a 7 mm diameter. The test was conducted in the compression mode of the software. The probe moved downwards with a speed of 1 mm/s and a trigger force of 0.049 N. The change in the length of the needle with an increase in the axial loading force was assessed.

2.2.8 *In vitro* permeation testing—*In vitro*** permeation studies were performed to determine the amount of NAC delivered into and across dermatomed human skin through various approaches. Vertical static Franz diffusion cells were utilized for the study that had a receptor chamber volume of 5 mL and a permeation area of 0.64 sq.cm (PermeGear, Inc., PA, USA). Various formulations containing NAC were applied to the skin in the donor chamber. NAC solution of 100 μL (15.96 %w/v), 100 μL of NAC gel (15.96% w/v), and 1 array of 10×10 fabricated NAC-loaded PVA sucrose microneedles (25.49 ± 0.03 mg of NAC/array) were applied on dermatomed human skin. The intact, non-microporated skin was used as a control to determine the permeation of NAC through passive diffusion. To keep sink conditions, 5mL of a 1X PBS solution (pH 7.4) was added to the receptor

chamber in accordance with the solubility of NAC in the receptor media. The skin surface temperature was maintained at 32 ± 1°C by keeping the receptor chamber at 37 ± 1°C by connecting it to an integrated water bath. The intact and microporated skin was positioned between the donor and receptor chambers. From the sampling arm of the receptor, 300 μL of receptor samples were taken at predetermined time points such as 0, 0.5, 1, 2, 4, 8, 22, and 24 h. It was immediately replaced with an equal volume of receptor solution to maintain the sink conditions after every sample. The receptor samples containing NAC delivered across the skin at each sampling time point were quantified using a validated high-performance liquid chromatography (HPLC) method.

2.2.9 Skin extraction studies—The amount of NAC delivered into the dermatomed human skin was determined by extracting it from the skin samples following the *in vitro* permeation studies. The unabsorbed formulation was removed from the skin using two cotton buds. The donor was removed, a new donor chamber was placed on the skin, and the skin was washed three times with 1 mL of 1X PBS solution to clean the unabsorbed NAC from the skin surface. The skin was dried with a dry cotton bud. The skin was then removed from the Franz cells, and the permeation area was cut and minced, and extracted with 2 mL of methanol as the extraction solvent for 4 h at 150 rpm on a platform shaker. The extracted drug concentrations were quantified using the validated HPLC method.

2.2.10 Quantitative analysis—The amount of NAC delivered into and across the skin from various formulations such as solution, gel, and drug-loaded microneedles was quantified using a validated High-Performance Liquid Chromatography (HPLC) method as described in our previous paper (Dandekar et al., 2023). Briefly, a Waters 2996 separation module with a UV photodiode array detector was used. The mobile phase composition of acetonitrile and 10 mM sodium dihydrogen phosphate (Na_2HPO_4), pH 7, was used in the ratio of 2:98 in an isocratic mode. A flow rate of 0.6 mL/min was maintained through an Agilent® Eclipse C18 column with dimensions 150 mm × 4.6 mm with a 5 μm particle size of stationary phase. The injection volume was 10 μL. The column temperature was maintained at 35°C. The detection wavelength was set at 210 nm. Empower 3 software was employed to process and display the results.

2.2.11 Lag time and flux determination—Lag time is considered as the time required for a drug to permeate across the skin into the receptor chamber. The cumulative amount of drug penetration over a unit area against a time plot was used to determine the most linear section, which was used to compute the lag time. We obtained a linear equation, and the lag time was estimated for the x variable by using zero as the substitute for the y variable value. The flux profile of NAC permeation was also generated as the amount of NAC permeated per unit area of the skin per unit of time and plotted against the time.

2.2.12 Statistical analysis—Study findings were presented as a mean and a standard error (SE). The software GraphPad Prism 9.3.1 (GraphPad Software, Inc., San Diego, CA) was used for all data analysis. The unpaired Mann-Whitney test was used to compute the statistical differences between the two groups, and a p-value of 0.05 or less was regarded as a significant difference. Statistical differences between three or more groups were calculated

using an ordinary one-way ANOVA test along with Tukey's test for multiple comparisons between each group unless otherwise stated; a p-value of ≤0.05 was regarded as a significant difference between the groups.

3 Results and discussion

3.1 Characterization studies

3.1.1 Rheological characteristics—Rheological parameters of the NAC-loaded gel were evaluated using a flow curve test and an amplitude sweep test. As seen in Fig. 1(A), the flow curve of 10% CMC gel showed a decrease in viscosity with an increase in shear rate. There was an increase in the shear stress with an increase in the shear rate observed. The NAC-loaded CMC gel displayed decreased viscosity as the shear rate increased. The amplitude sweep indicated that the loss modulus was higher than the storage modulus of the gel, with an increase in the strain, as observed in Fig. 1(B).

3.1.2 Scanning electron microscopy (SEM) studies—The fabricated PVA sucrose microneedles, as well as the NAC-loaded microneedles, were examined using SEM studies. As illustrated in Fig. 2A, the SEM images of blank microneedles displayed pyramidal-shaped microneedles with an average needle length of 387.31 ± 8.94 μm (n=5), whereas the drug-loaded microneedles were 409.16 ± 6.04 μm (n=5), as appeared in Fig. 2B and 2C. The needle-to-needle distance of blank and drug-loaded microneedles was reported to be 504.50 ± 3.24 μm (n=5) and 516.87 ± 10.82 μm (n=5), respectively. The average base side of the blank microneedles was found to be 115.97 ± 0.73 μm (n=5), whereas the drug-loaded microneedles were found to be 127.62 ± 3.87 μm (n=5). Fig. 2D depicts skin that has been microporated using the fabricated microneedles.

3.1.3 Skin integrity test—After using the fabricated microneedles to microporate the skin, the observed electrical resistance of the skin was significantly decreased ($p = 0.0002$), as seen in Fig.3.

3.1.4 Histology studies of the microporated skin—Histology studies were conducted to visualize the skin microporation caused by the application of the microneedles. The studies indicated that microneedles caused a disruption in the stratum corneum as compared to the continuous and unabraded stratum corneum in the intact skin. The microchannels created were around 100 μm in-depth, as seen in Fig.4B. As seen in Fig. 4B, the fabricated microneedles penetrated the stratum corneum and the epidermal region, and not the dermis region where the nerve endings are typically present.

3.1.5 Confocal Laser Microscopy Studies—Following the use of fabricated microneedles, the depth of the microchannels that were formed was examined employing confocal laser microscopy. To estimate the overall depth, a Z-stack was recorded with a step count of 10 μm. As illustrated in Fig 5., the depth of the microchannels produced by the microneedles was 120 μm.

3.1.6 Mechanical strength test—The fabricated placebo PVA-sucrose microneedles, as well as NAC-loaded microneedles, were subjected to mechanical strength testing with

axial loading. The axial loading force required to deform the placebo needles was found to be 63.72 N/array for an array of 100 needles, and NAC-loaded microneedles were found to be 63.58 N/array. Thus, the addition of NAC on the microneedles did not significantly affect the mechanical strength of the microneedles.

3.2 *In vitro* permeation testing

In vitro permeation studies were carried out on dermatomed human skin. There were no detectable amounts of NAC in the receptor or the skin samples through passive permeation. As seen from the results in Fig. 6, microporation resulted in a significant increase in the delivery of NAC. The total delivery via poke and solution, poke and gel, and drug-loaded microneedles was 509.84 ± 155.04 μg/sq.cm 474.91 ± 70.09 μg/sq.cm, and 226.89 ± 33.41 μg/sq.cm respectively.

3.3 Skin extraction studies

The skin extraction study results indicated no skin delivery of NAC via passive permeation. Upon microporation using the PVA sucrose microneedles, the skin delivery of NAC significantly increased up to 69.98 ± 17.40 μg/sq.cm, as seen in Fig 6B. The skin delivery using poke and gel application was found to be 33.67 ± 6.19 μg/sq.cm, whereas that from the application of drug-loaded microneedles was found to be 33.53 ± 5.40 μg/sq.cm.

3.4 Flux profile and lag time determination

The flux profile of NAC delivery is shown in Fig. 7A. Amongst the microneedle-treated groups, the highest flux was observed for the poke and solution group, followed by the poke-and-gel group up to 2 h, followed by a steady decrease in the flux up to 24 h. The lag time for NAC delivery through passive permeation was not calculated as NAC did not permeate through intact skin. However, microporated skin was found to be 0.23 ± 0.04 h 0.25 ± 0.04 h, and 0.25 ± 0.02 h, respectively as seen in Fig. 7B, whereas the lag time for the delivery of NAC through the application of NAC-loaded microneedles was found to be 1.27 ± 1.16 h.

4. Discussion

Accidental exposure of Lewisite to the civilian population can result in a public health emergency, as Lewisite is a highly toxic skin blistering agent. Besides British anti-Lewisite (BAL), which is toxic with low efficacy, there is no other more efficacious antidote against Lewisite. In our previous studies, we have recognized N-acetyl cysteine as one of the potential antidotes for the treatment of Lewisite-mediated skin injury. The activity of NAC has been tested *in vivo* with mice models using phenyl arsine oxide (PAO), which has been developed as a surrogate molecule to Lewisite (Li et al., 2016b). We demonstrated that N-acetyl cysteine, an antioxidant molecule, can reduce PAO-induced skin injury in the skin. In our previous studies, we have also explored the feasibility of delivering NAC into the skin, including the use of chemical enhancers as well as physical enhancement techniques such as iontophoresis (Dandekar et al., 2023). In the present study, we have demonstrated for the first time the feasibility of delivering NAC using microneedle formulations as a physical enhancement technique. We explored three approaches- poke and solution, poke and gel,

and NAC-loaded microneedles for the delivery of NAC and studied it's *in vitro* permeation across dermatomed human skin.

The physicochemical properties of a formulation can significantly affect drug delivery. Amongst them, pH plays a vital role in the passive permeation of molecules into and across the skin, as the unionized form of a molecule can permeate more than the ionized form(Banga, 2011). NAC being hydrophilic in nature, showed no detectable amounts across dermatomed human skin, which can be attributed to its ionization in the vehicle. However, skin microporation resulted in an overall increase in the delivery of NAC into and across the skin. The *in vitro* permeation of NAC solution across microporated skin was found to be highest, followed by gel and, finally, the NAC-loaded microneedles. NAC delivery could have been highest from the PBS vehicle also due to the neutral charge on the molecule at a highly acidic pH value in the PBS vehicle, followed by the CMC gel, which was at neutral pH, resulting in overall ionization of NAC in the gel, thereby reducing its transdermal delivery as compared to PBS vehicle (ChemAxon, 2022). This difference in pH of the formulations could have contributed to the transdermal delivery of NAC across intact and microporated skin.

In addition to the pH, the difference in permeation can be attributed to the physical formulation characteristics, where delivery from a solution is expected to have the highest delivery compared to a gel or polymeric microneedles, which can delay the permeation. Rheological studies performed with NAC gel depicted an increase in the shear stress with an increase in shear rate observed, indicating that the NAC gel showed shear thinning behavior. Ideal semisolid formulations such as gels should have higher structural stability during storage and shear-thinning properties while being dispensed from containers and spreading on the skin (Vora et al., 2021). The NAC-loaded CMC gel displayed similar properties as the viscosity decreased as the shear rate increased. The property of a hydrogel to store deformation energy in an elastic way is termed the storage modulus (G'). The storage modulus of a formulation increases with increasing crosslinking. On the other hand, the loss modulus (G") reflects the polymer's capacity to release stress through the ratio of the viscous component to the stress (Anseth et al., 1996). The amplitude sweep indicated that the loss modulus was higher than the storage modulus, indicating that the gel is more viscous than elastic. CMC is a cellulose-based polymer where the degree of substitution and method of preparing the gel significantly influences the rheological parameters. The observation obtained is consistent with the literature stating that CMC with uniform substitutions leads to the formation of pseudoplastic solutions (Elliot and Ganz, 1974).

The fabricated PVA sucrose microneedles, as well as the NAC-loaded microneedles, were examined using SEM studies. The microneedle length obtained was consistent with our previously fabricated microneedles with the same master template geometry (Kale et al., 2020). The difference in the microneedle length between blank and drug-loaded microneedles can be attributed to the slight differences in the viscosities of the polymer blends (Nguyen et al., 2018; Yang et al., 2012). The addition of NAC could have affected the viscosity of the solution, leading to the effective filling of the PDMS mold during vacuum application. The distance between the needles and the base side observed is

consistent with the observations in our previous studies(Nguyen and Banga, 2017). The SEM data suggests that the fabricated microneedles were visually uniform in shape with sharp tips, creating microchannels successfully upon insertion into the skin. Skin barrier integrity disruption is an indication that microporation has been successful, as observed in our present study. The stratum corneum barrier layer is damaged when microneedles are used, which lowers the skin's electrical resistance due to an increase in the conductance caused due to microporation (Lanke et al., 2009). Observing a drop in electrical resistance upon disruption of stratum corneum by microneedle application has been reported several times in the literature. (Dandekar et al., 2022b; Kshirsagar et al., 2022) Histology studies indicated that microneedles caused a disruption in the stratum corneum in the form of abrasion and deformation compared to the continuous and unabraded stratum corneum in the intact skin, thereby supporting the observation of lowered electrical resistance. The actual depth of microneedles after the application was less than the height of microneedles. This observation is consistently reported in several other in vitro studies where a depth of only 10 to 30% of the original needle length was observed(Kalluri and Banga, 2011; Lanke et al., 2009). Several factors, such as skin elasticity and resistance to applied force, can contribute to incomplete insertion. The study indicated that the fabricated microneedles penetrated the stratum corneum and the epidermal region, not the dermis region where the nerve endings are typically present, thus making the administration painless and minimally invasive. However, the reduced depth of insertion of microneedles observed during histology studies can be due to the physical distortion that can alter the dimensions(Nguyen et al., 2018). Nevertheless, the breach of the stratum corneum was confirmed by observing a decrease in the electrical resistance upon skin microporation, similar to previously reported studies (Kshirsagar et al., 2022; Nguyen and Banga, 2015). Additionally, the depth observed in confocal microscopy correlated with the results obtained from histology studies. These results were expected where the penetration depth was lower than the microneedle length, as the skin's viscoelastic nature provided resistance to penetration. We have seen similar results in some of our previous studies as well(Nguyen and Banga, 2017). Other than skin-related factors, pressure and duration of microneedle application can have a significant impact on the penetration depth of the microneedles(Xiu et al., 2022). Moreover, the mechanical strength of microneedles can significantly affect the skin's microporation ability. Previously, Davis et al. reported the force of microneedle fracture to be a sudden drop in the axial force applied on the microneedles caused due to fracture of microneedles (Davis et al., 2004). The outcome of the mechanical strength study demonstrated that when the spindle was pushed on the microneedles, the axial force increased continuously with the spindle's travel distance. The addition of NAC on the microneedles did not significantly affect the mechanical strength of the microneedles. Zhang et al. developed PVA sucrose microneedles for insulin delivery and reported a lower fracture force of up to 0.2 N/needle (Zhang et al., 2021). The mechanical strength of microneedles can be significantly influenced by the microneedle geometry and composition (Anjani et al., 2021). Polymeric microneedles generally have lower mechanical strength as compared to metal, silicon, ceramic, or glass but have a better safety profile (Larrañeta et al., 2016). The use of biodegradable polymers like PVA and dissolvable sugar like sucrose can mitigate the issue of safety upon microneedle insertion into the skin (Chu and Prausnitz, 2011).

The differences observed in the *in vitro* permeation studies in terms of total delivery among the three microporation approaches are expected, considering the mechanism of drug diffusion in every process. The dose of NAC used in this study was based on our previous studies conducted *in vivo* in mice, demonstrating safety and effectiveness(Dandekar et al., 2023). Poke and solution showed the highest delivery wherein the drug dissolved in an aqueous solution could quickly diffuse via the hydrophilic microchannels. The delivery was slightly reduced when moving to a poke and gel, wherein the viscous nature of gel led to a comparatively slower release of the drug. Finally, the drug-loaded microneedles showed the lowest delivery, which can be attributed to the diffusion of the drug from microneedles into microchannels and then across the skin. In addition, the drug-loaded microneedles are also limited by the amount of drug that can be loaded in the array. To ensure maximum loading for comparison, we loaded NAC in both the needles and the backing layer in this study, thus increasing the drug loading to 25 mg per array. Despite the slight differences in the drug loading between poke and application and drug-loaded groups, all three approaches successfully delivered NAC into and across dermatomed human skin. The poke-solution and poke-gel approaches can achieve higher drug loading and hence higher delivery but will require a two-step application process. Drug-loaded microneedles are limited by their drug-loading capacity but can offer better patient compliance as they can be self-administered in a single step. Overall, the results suggest that microporation is a promising approach for the delivery of NAC via skin. The trend of the amount of NAC in the skin was similar to receptor delivery, where poke and solution resulted in the highest delivery, with skin delivery via poke and gel and drug-loaded microneedles being similar. The difference can be attributed to the physical nature of the formulation applied on the skin, where aqueous solution showed maximum skin delivery and solid drug-loaded microneedles showed the least amount. Skin delivery of NAC is essential for the local mitigation of arsenical-based skin injuries. With microneedles, a significant amount of antioxidant NAC can be delivered into the skin for local effect.

The flux profile for NAC delivery is shown in Fig.7A, where no transdermal permeation and flux were observed for passive delivery of NAC. Amongst the microneedle-treated groups, the highest flux was observed for the poke and solution group, followed by the poke and gel group up to 2 h, followed by a steady decrease in the flux up to 24 h. The flux for NAC-loaded microneedles steadily increased up to 4 h and showed a decline up to 24 h. The differences in achieving the highest flux can be attributed to the time needed for drug diffusion via the three approaches. Hence, poke and solution and poke and gel resulted in similar flux profiles, whereas drug-loaded microneedles showed a slower rate of drug diffusion. These results were correlated to the calculated lag time as well. The lag time for NAC delivery through passive permeation was not calculated as NAC did not permeate through intact skin. However, the lag time for NAC delivery through the application of NAC solution and NAC gel on microporated skin was found to be 0.23 ± 0.04 h and 0.25 ± 0.02 h, respectively, as seen in Fig 7B, whereas the lag time for the delivery of NAC through the application of NAC-loaded microneedles was found to be 1.27 ± 1.16 h. A shorter lag time is desirable for faster onset of action. Thus, the poke and solution or poke and gel approach resulted in faster and higher delivery as compared to the drug-loaded microneedle approach. Similar results were obtained by Nguyen et al. for the delivery of doxorubicin via various

microporation approaches(Nguyen et al., 2018). Therefore, depending on desired delivery and practical application considerations, one of three approaches can be employed to achieve successful transdermal delivery and tailor the release of NAC for arsenical-mediated skin injury.

5. Conclusion

The present study explored skin microporation as an approach for physically enhancing the transdermal delivery of N-acetyl cysteine, an antioxidant, for the treatment of arsenical-mediated skin injury. Poke and solution, poke and gel, as well as the drug-loaded microneedles approach, resulted in enhanced delivery of NAC into and across dermatomed human skin, establishing the feasibility of using this approach for rapid delivery of NAC via skin.

Funding

This project was funded by NIH/NIAMS 1U01AR078544 to M.A. The study sponsors were not involved in the study design, data collection, analysis, data interpretation, manuscript writing, or the decision to publish the manuscript.

Abbreviations:

NAC	N-Acetylcysteine
MW	Molecular Weight
FDA	Food and Drug Administration
BAL	British Anti-Lewisite
ROS	Reactive Oxygen Species
PAO	Phenyl Arsine Oxide
CMC	Carboxymethyl Cellulose sodium salt
PVA	Polyvinyl Alcohol
HPLC	High-Performance Liquid Chromatography
PDMS	Poly Dimethyl Siloxane
SEM	Scanning Electron Microscopy
PBS	phosphate buffered saline
ANOVA	Analysis of variance

6. References

Aldawood FK, Andar A, Desai S, 2021. A comprehensive review of microneedles: Types, materials, processes, characterizations and applications. Polymers (Basel). 10.3390/polym13162815

Anjani QK, Permana AD, Cárcamo-Martínez Á, Domínguez-Robles J, Tekko IA, Larrañeta E, Vora LK, Ramadon D, Donnelly RF, 2021. Versatility of hydrogel-forming microneedles in in vitro transdermal delivery of tuberculosis drugs. European Journal of Pharmaceutics and Biopharmaceutics 158, 294–312. 10.1016/j.ejpb.2020.12.003 [PubMed: 33309844]

Anseth KS, Bowman CN, Brannon-Peppas L, 1996. REVIEW Mechanical properties of hydrogels and their experimental determination, Biomoterjols.

Banga AK, 2011. Transdermal and Intradermal Delivery of Therapeutic Agents-Applications of Physical Technologies. CRC Press.

Banga AK, 2009. Microporation applications for enhancing drug delivery. Expert Opin Drug Deliv. 10.1517/17425240902841935

Centers for Disease Control and Prevention, 2018. Facts about Lewisite [WWW Document]. URL https://emergency.cdc.gov/agent/lewisite/basics/facts.asp (accessed 2.11.23).

ChemAxon, 2022. Chemicalize-Instant Cheminformatics Solutions | N-acetyl cysteine [WWW Document]. URL https://chemicalize.com/app/calculation/nacetylcysteine (accessed 12.15.22).

Chu LY, Prausnitz MR, 2011. Separable arrowhead microneedles. Journal of Controlled Release 149, 242–249. 10.1016/j.jconrel.2010.10.033 [PubMed: 21047538]

Dandekar A, Vora D, Yeh JS, Srivastava RK, Athar M, Banga AK, 2023. Enhanced Transdermal Delivery of N-acetylcysteine and 4-phenylbutyric acid for Potential Use as Antidotes to Lewisite AAPS PharmSciTech. AAPS PharmSci Tech.

Dandekar AA, Garimella HT, German CL, Banga AK, 2022a. Microneedle Mediated Iontophoretic Delivery of Tofacitinib Citrate. Pharm Res. 10.1007/s11095-022-03190-5

Dandekar AA, Kale M, Garimella HT, Banga AK, 2022b. Effect of compromised skin barrier on delivery of diclofenac sodium from brand and generic formulations via microneedles and iontophoresis. Int J Pharm 628, 122271. 10.1016/J.IJPHARM.2022.122271 [PubMed: 36220591]

Davis SP, Landis BJ, Adams ZH, Allen MG, Prausnitz MR, 2004. Insertion of microneedles into skin: Measurement and prediction of insertion force and needle fracture force. J Biomech 37, 1155–1163. 10.1016/j.jbiomech.2003.12.010 [PubMed: 15212920]

Delnomdedieu M, Basti M, Otvos JD, Thomas JD, 1993. Transfer of arsenite from glutathione to dithiols: a model of interaction. Chem Res Toxicol. 598–602. [PubMed: 8292735]

Elliot JH, Ganz AJ, 1974. Some rheological properties of sodium carboxymethylcellulose solutions and gels*), Rheol. Acta.

Flora SJS, Flora G, Saxena G, 2009. Arsenicals: Toxicity, their use as chemical warfare agents, and possible remedial measures, in: Handbook of Toxicology of Chemical Warfare Agents. Elsevier Inc., pp. 109–133. 10.1016/B978-0-12-374484-5.00009-2

Fox ER, Johnson-Arbor K, Mazer-Amirshahi M, 2021. Will There Ever be an Antidote for Drug Shortages? Journal of Medical Toxicology 321–322. 10.1007/s13181-021-00830-x/Published [PubMed: 33687652]

Giudice EL, Campbell JD, 2006. Needle-free vaccine delivery. Adv Drug Deliv Rev 58, 68–69. [PubMed: 16564111]

Guillot AJ, Cordeiro AS, Donnelly RF, Montesinos MC, Garrigues TM, Melero A, 2020. Microneedle-based delivery: An overview of current applications and trends. Pharmaceutics. 10.3390/pharmaceutics12060569

Junaid MSA, Banga AK, 2022. Transdermal Delivery of Baclofen Using Iontophoresis and Microneedles. AAPS PharmSciTech 23, 84. 10.1208/s12249-022-02232-w [PubMed: 35288825]

Kale M, Kipping T, Banga AK, 2020. Modulated delivery of donepezil using a combination of skin microporation and iontophoresis. Int J Pharm 589. 10.1016/j.ijpharm.2020.119853

Kalluri H, Banga AK, 2011. Formation and closure of microchannels in skin following microporation. Pharm Res 28, 82–94. 10.1007/s11095-010-0122-x [PubMed: 20354766]

Kshirsagar SM, Kipping T, Banga AK, 2022. Fabrication of Polymeric Microneedles using Novel Vacuum Compression Molding Technique for Transdermal Drug Delivery. Pharm Res. 10.1007/s11095-022-03406-8

Lanke SSS, Kolli CS, Strom JG, Banga AK, 2009. Enhanced transdermal delivery of low molecular weight heparin by barrier perturbation. Int J Pharm 365, 26–33. 10.1016/j.ijpharm.2008.08.028 [PubMed: 18801420]

Larrañeta E, Lutton REM, Woolfson AD, Donnelly RF, 2016. Microneedle arrays as transdermal and intradermal drug delivery systems: Materials science, manufacture and commercial development. Materials Science and Engineering R: Reports. 10.1016/j.mser.2016.03.001

Li C, Srivastava RK, Athar M, 2016a. Biological and environmental hazards associated with exposure to chemical warfare agents: arsenicals. Ann N Y Acad Sci 1378, 143–157. 10.1111/nyas.13214 [PubMed: 27636894]

Li C, Srivastava RK, Weng Z, Croutch CR, Agarwal A, Elmets CA, Afaq F, Athar M, 2016b. Molecular Mechanism Underlying Pathogenesis of Lewisite-Induced Cutaneous Blistering and Inflammation: Chemical Chaperones as Potential Novel Antidotes. American Journal of Pathology 186, 2637–2649. 10.1016/j.ajpath.2016.06.012 [PubMed: 27528504]

Mouret S, Wartelle J, Emorine S, Bertoni M, Nguon N, Cléry-Barraud C, Dorandeu F, Boudry I, 2013. Topical efficacy of dimercapto-chelating agents against lewisite-induced skin lesions in SKH-1 hairless mice. Toxicol Appl Pharmacol 272, 291–298. 10.1016/j.taap.2013.06.012 [PubMed: 23806213]

National Institute of Health, 2007. NIH Strategic Plan and Research Agenda for Medical Countermeasures Against Chemical Threats.

Nguyen HX, Banga AK, 2017. Fabrication, characterization and application of sugar microneedles for transdermal drug delivery. Ther Deliv 8, 249–264. 10.4155/tde-2016-0096 [PubMed: 28361607]

Nguyen HX, Banga AK, 2015. Enhanced skin delivery of vismodegib by microneedle treatment. Drug Deliv Transl Res 5, 407–423. 10.1007/s13346-015-0241-3 [PubMed: 26069156]

Nguyen HX, Bozorg BD, Kim Y, Wieber A, Birk G, Lubda D, Banga AK, 2018. Poly (vinyl alcohol) microneedles: Fabrication, characterization, and application for transdermal drug delivery of doxorubicin. European Journal of Pharmaceutics and Biopharmaceutics 129, 88–103. 10.1016/j.ejpb.2018.05.017 [PubMed: 29800617]

NIOSH, CDC, 2011. Lewisite (L): Blister Agent (https://www.cdc.gov/niosh/ershdb/emergencyresponsecard_29750006.html) [WWW Document]. URL https://www.cdc.gov/niosh/ershdb/emergencyresponsecard_29750006.html (accessed 7.8.23).

Shrestha N, Banga AK, 2022. Development and evaluation of transdermal delivery system of tranylcypromine for the treatment of depression. Drug Deliv Transl Res. 10.1007/s13346-022-01269-5

Vora D, Banga AK, 2022. Development and evaluation of a drug-in-adhesive transdermal delivery system for delivery of olanzapine. Expert Opin Drug Deliv 19, 1539–1548. 10.1080/17425247.2022.2135700 [PubMed: 36242524]

Vora D, Dandekar AA, Srivastava RK, Athar M, Banga AK, 2022a. Development and Evaluation of a Topical Foam Formulation for Decontamination of Warfare Agents. Mol Pharm. 10.1021/acs.molpharmaceut.2c00636

Vora D, Garimella HT, German CL, Banga AK, 2022b. Microneedle and iontophoresis mediated delivery of methotrexate into and across healthy and psoriatic skin. Int J Pharm 618, 121693. 10.1016/j.ijpharm.2022.121693 [PubMed: 35331833]

Vora D, Kim Y, Banga AK, 2021. Development and evaluation of a heparin gel for transdermal delivery via laser-generated micropores. Ther Deliv 12, 133–144. 10.4155/tde-2020-0024 [PubMed: 33496196]

Watson AP, Griffin GD, 1992. Toxicity of Vesicant Agents Scheduled for Destruction by the Chemical Stockpile Disposal Program, Environmental Health Perspectives.

Xiu X, Gao G, Liu Y, Ma F, 2022. Drug delivery with dissolving microneedles: skin puncture, its influencing factors and improvement strategies. J Drug Deliv Sci Technol. 10.1016/j.jddst.2022.103653

Yang S, Feng Y, Zhang L, Chen N, Yuan W, Jin T, 2012. A scalable fabrication process of polymer microneedles. Int J Nanomedicine 7, 1415–1422. 10.2147/IJN.S28511 [PubMed: 22457598]

Zhang N, Zhou X, Liu L, Zhao L, Xie H, Yang Z, 2021. Dissolving Polymer Microneedles for Transdermal Delivery of Insulin. Front Pharmacol 12. 10.3389/fphar.2021.719905

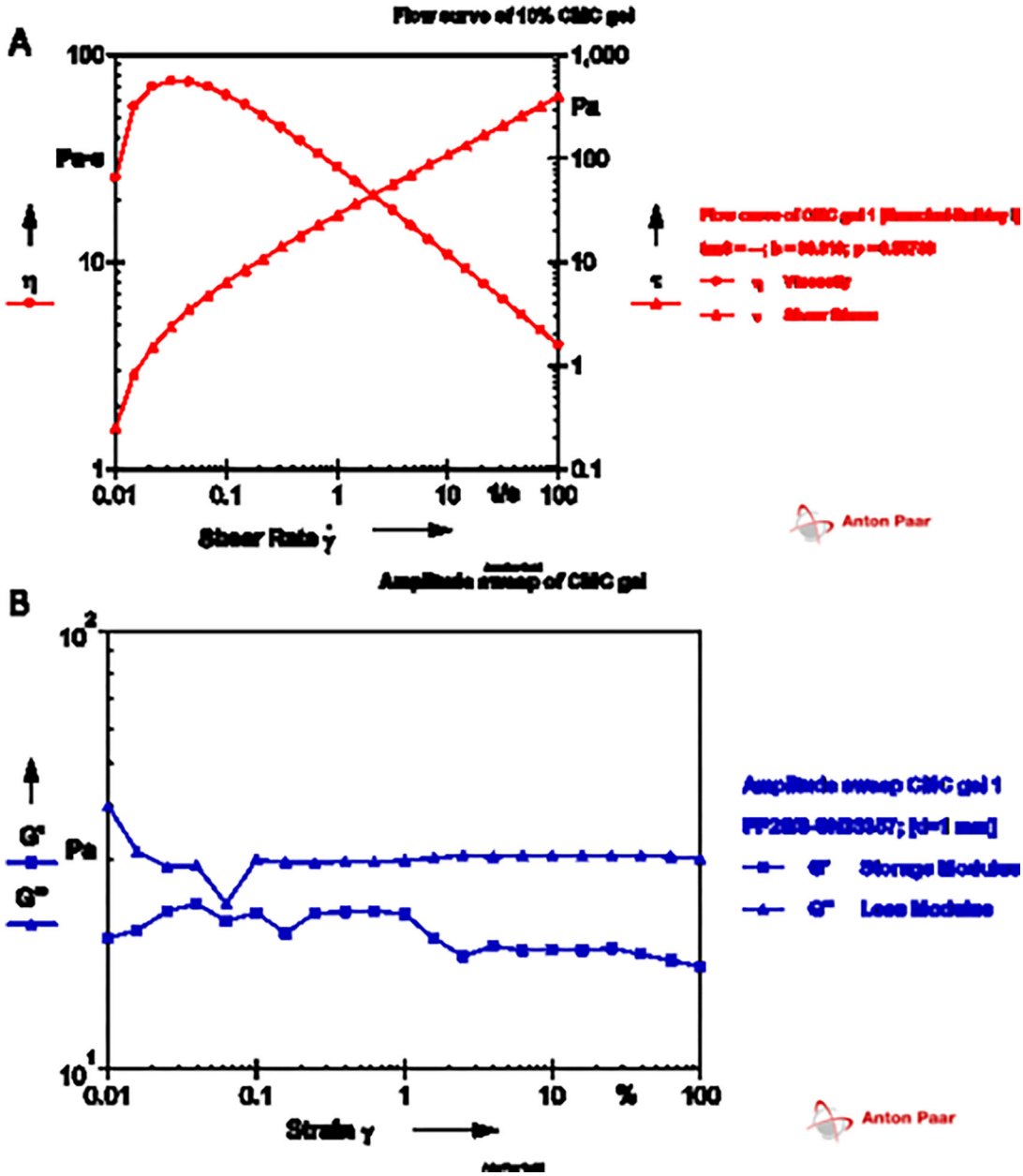

Fig. 1.

Rheological analysis of NAC-loaded CMC gel showing (A) flow curve test with the effect of shear stress on viscosity (η) and shear rate (τ); and (B) amplitude sweep test to determine the viscoelastic nature of the gel

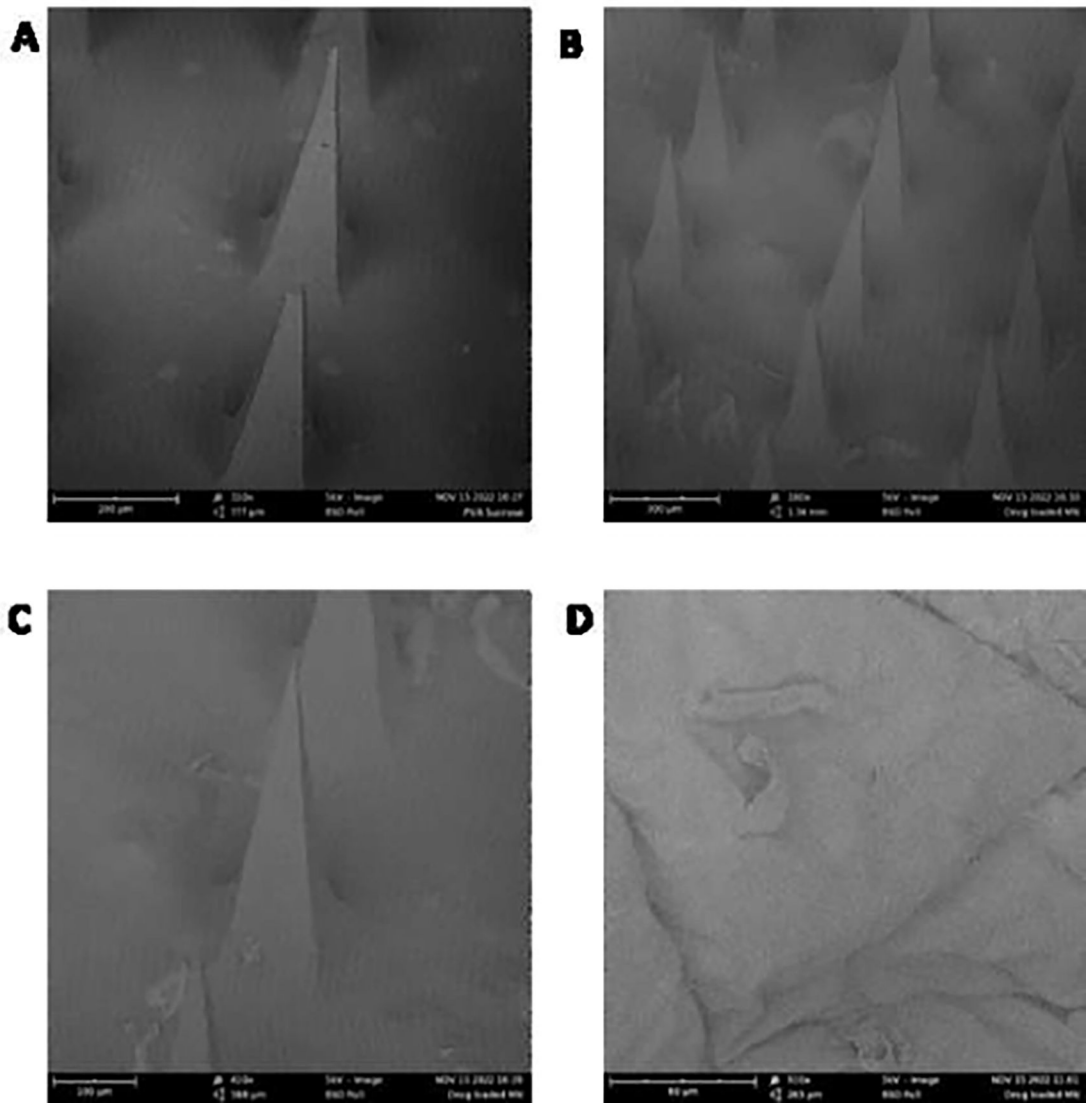

Fig. 2.

Scanning electron microscopy images of (A) blank microneedles, scale bar represents 200 μm and magnification of 310x (B) drug-loaded microneedles, scale bar represents 300 μm and magnification of 180x (C) single drug-loaded microneedle, scale bar represents 100 μm and magnification of 410x (D) microporated dermatomed human skin, scale bar represents 80 μm and magnification of 910x

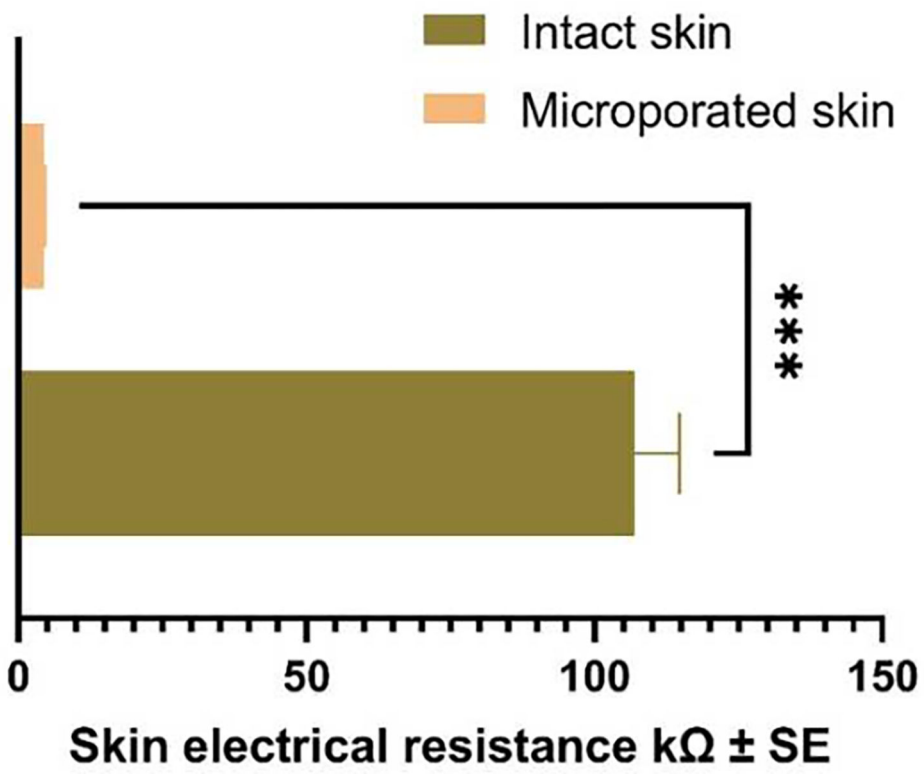

Fig. 3.

Drop in the trans-epidermal electrical resistance of the skin upon microporation with microneedles. Statistical analysis was performed using Mann-Whitney's test; *** indicates a significant difference between the groups $p<0.001$

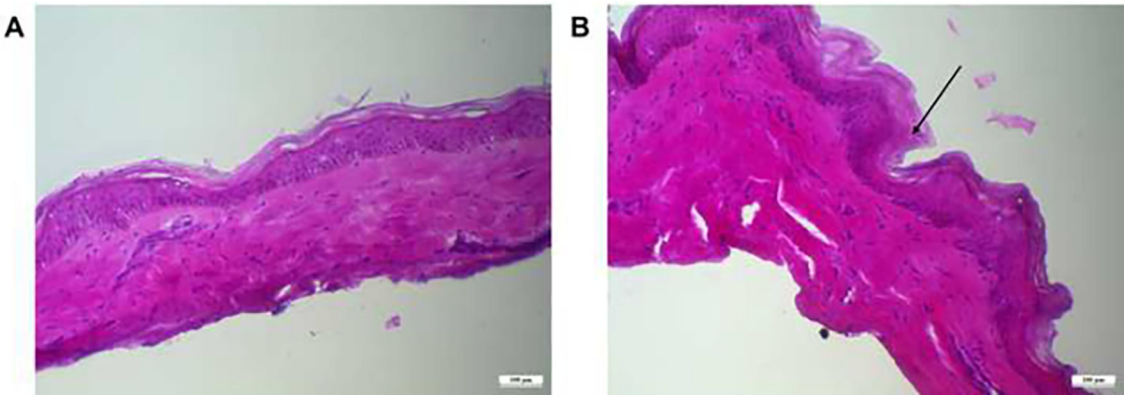

Fig. 4.

Histology section of (A) intact dermatomed human skin and (B) skin microporated with microneedles, scale bar represents 100 μm.

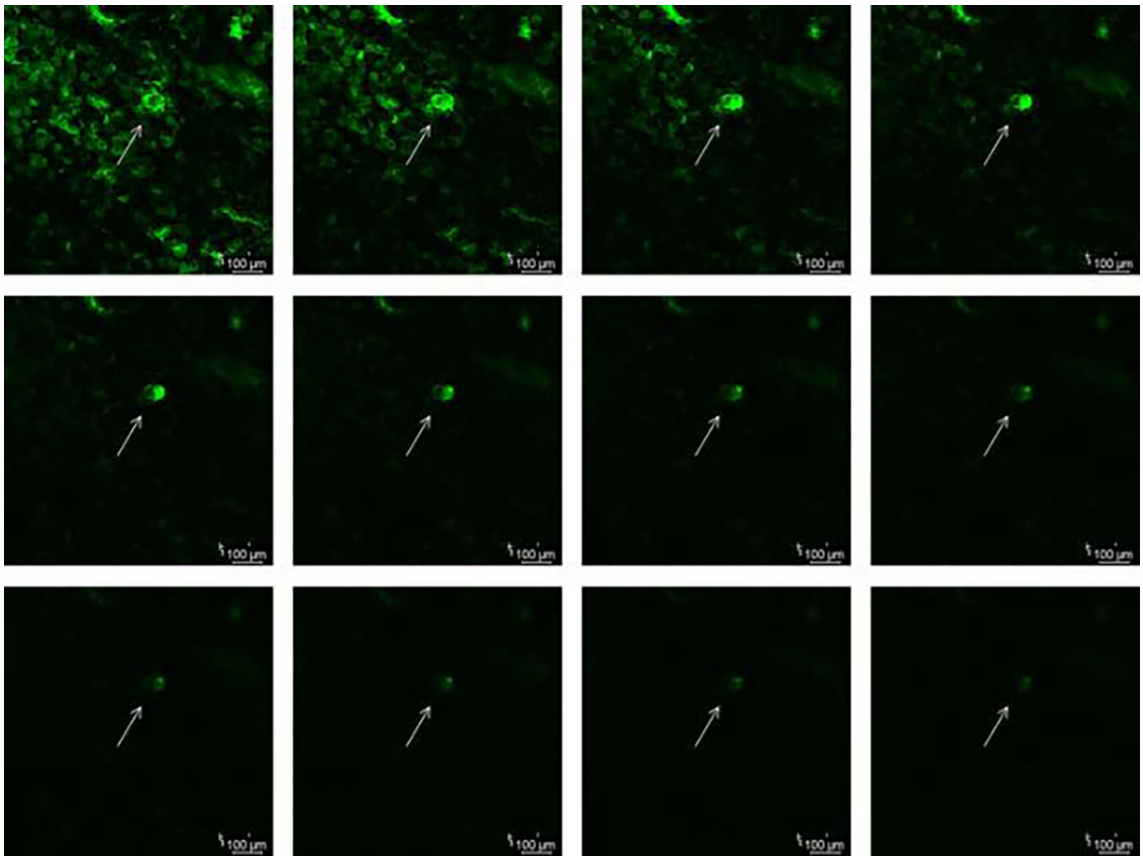

Fig. 5.

Z-stack of the microporated skin showing the depth of microneedles using confocal laser microscopy with a step count of 10 μm

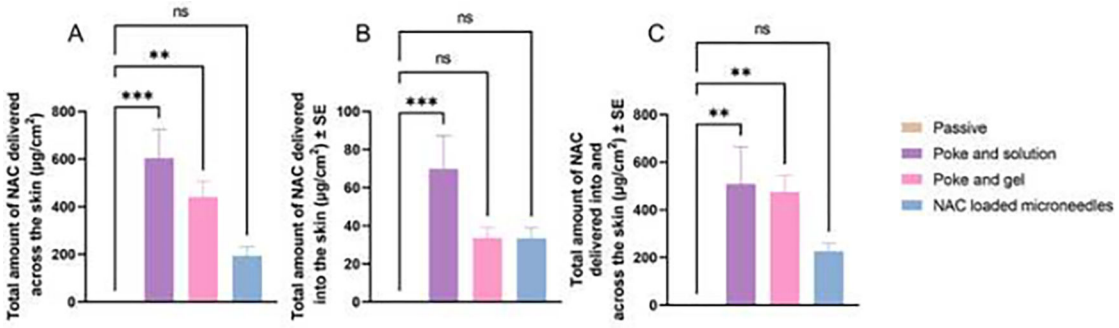

Fig. 6.

(A) *In vitro* permeation of NAC into the receptor compartment expressed as µg/cm^2, (B) Amount of NAC accumulated in the skin tissue up to 24 h, (C) Total amount of NAC delivered into and across the skin up to 24 h. Statistical significance expressed using ordinary one-way ANOVA test, *** indicates a significant difference between the groups ($p<0.001$); ** indicates a significant difference between the groups ($p<0.01$); * indicates a significant difference between the groups ($p<0.05$); ns indicates no significant difference between the groups.

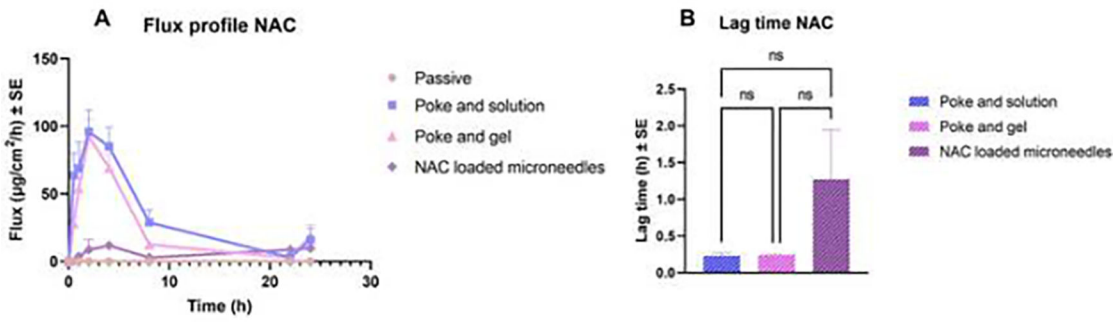

Fig. 7.

(A) Flux profile for N-acetyl cysteine delivery across the skin, (B) lag time for the delivery of NAC into the receptor compartment